Preliminary Orbit Determination from Self-Contained Data

ROBERT H GERSTEN* AND Z E SCHWARZBEIN†
Northrop Space Laboratories, Hawthorne, Calif

Introduction

IN two previous papers[1,2] the authors have established several mathematical models for self-contained preliminary orbit determination (with all computations and measurements made on board) As discussed in detail in Ref 1, the orientation of the orbit plane in inertial space and the increment in true anomaly between the first and succeeding measurements can be obtained from observations of landmarks of the principal body (under the assumption that the body-centered latitude and longitude of these landmarks, as well as the rotation rate of the principal body, are known) or stellar observations Once the orientation of the orbit plane and increment in true anomaly have been determined, the two-body orbital elements can be obtained from A) three additional measurements and the associated times (without recourse to time of flight equations), or B) two additional measurements and the time of flight (utilizing time of flight equations) Reference 1 considers orbit determination of type A from the following data combinations: 1) three measurements of either the altitude, radial velocity, or time rate of change of true anomaly and the associated times; and 2) two measurements of any one of the preceding quantities, the first of which is taken simultaneously with the measurement of one of the other quantities Reference 2 considers a class of orbit determination falling under type B (orbit determination from two measurements of radial velocity and the time of flight) The present paper considers the extension of type B to include self-contained orbit determination from two measurements of either altitude or time rate of change of true anomaly and the time-of-flight equations Since oblateness effects and local anomalies are neglected in this analysis, altitude and radial velocity can be obtained directly from measurements of range and range-rate along the local vertical of the principal body Likewise, time rate of change of true anomaly is obtained from successive determinations of the direction of the local vertical Of course, the vehicular separation from the dynamical center is equal to the sum of the altitude and the (assumed constant) radius of the principal body

Derivation

1 Two measurements of altitude and time-of-flight equations

The orientation of the orbit plane can be obtained through a determination of the unit vectors $\mathbf{U}_1$, $\mathbf{U}_2$, directed from the origin (at the dynamical center of the principal body) to the satellite at the observation times, by a method discussed in Ref 1, where subscripts 1 and 2 correspond to the first and second observations, respectively Having two measurements of altitude, one can obtain the vehicular vector separations from the dynamical center at the observations time $\mathbf{r}$ directly from

$$\mathbf{r}_j = r_j \mathbf{U}_j \qquad j = 1, 2 \tag{1}$$

where r is the magnitude of $\mathbf{r}$ (equal to the sum of the measured altitude and the assumed constant radius of the principal body) The case of orbit determination from two $\mathbf{r}$'s and the included time of flight is identical to the classical Gaussian method A modification of this method, requiring iteration on assumed values of the parameter p (semilatus rectum), developed by Herrick and Liu,[3-5] is particularly useful for determination of orbits of artificial satellites Since this method is well discussed in the literature, it will not be treated here

2 Two measurements of time rate of change of true anomaly and time-of-flight equations

The case of orbit determination from two measurements of time rate of change of true anomaly and the time of flight requires a little more analysis Having determined $\mathbf{U}_1$ and $\mathbf{U}_2$, as well as the increment in true anomaly between the first and second measurements, Δv (this last being obtained via the relationship $\Delta v = \arccos(\mathbf{U}_1 \cdot \mathbf{U}_2)$ under the assumption $0 < \Delta v < \pi$), the next task is the determination of the parameter p (semilatus rectum), orbital eccentricity e, and true anomaly at the first observation time v_1 The time rate of change of true anomaly $\dot{v}$ is given by

$$\dot{v}_1 = (\mu/p^3)^{1/2}(1 + e\cos v_1)^2 \tag{2a}$$

$$\dot{v}_2 = (\mu/p^3)^{1/2}[1 + e\cos(v_1 + \Delta v)]^2 \tag{2b}$$

where μ is the product of the universal gravitational constant and the mass of the principal body

Equations (2) yield, after some manipulation,

$$e\sin v_1 = [1 - \cos\Delta v - P(\dot{V}_2 - \dot{V}_1\cos\Delta v)]/\sin\Delta v \tag{3a}$$

$$e\cos v_1 = P\dot{V}_1 - 1 \tag{3b}$$

where

$$P = (p^3/\mu)^{1/4} \qquad \dot{V} = \dot{v}^{1/2} \tag{3c}$$

The time-of-flight equations for elliptical, parabolic, and hyperbolic orbits are, respectively,[6]

$$t_2 - t_1 = \frac{P^2}{1 - e^2}\left\{\frac{-e\sin v}{1 + e\cos v} + \frac{2}{(1 - e^2)^{1/2}}\tan^{-1}\left[\left(\frac{1 - e}{1 + e}\right)^{1/2}\tan\frac{v}{2}\right]\right\}\Bigg|_{v_1}^{v_2 = v_1 + \Delta v} \tag{4a}$$

$$t_2 - t_1 = \frac{1}{2}P^2\tan\frac{v}{2}\left(1 + \frac{1}{3}\tan^2\frac{v}{2}\right)\Bigg|_{v_1}^{v_2 = v_1 + \Delta v} \tag{4b}$$

$$t_2 - t_1 = \frac{P^2}{1 - e^2}\left\{\frac{-e\sin v}{1 + e\cos v} + \frac{2}{(e^2 - 1)^{1/2}}\tanh^{-1}\left[\left(\frac{e - 1}{e + 1}\right)^{1/2}\tan\frac{v}{2}\right]\right\}\Bigg|_{v_1}^{v_2 = v_1 + \Delta v} \tag{4c}$$

where t represents the time Equations (3a), (3b), and the proper one of Eqs (4) constitute three equations in three unknowns: P, e, and v_1 The solution can proceed as follows Assuming a value of P, Eqs (3a) and (3b) give e and v_1 directly (the former by taking the positive square root of the sum of the squares of Eq (3a) and (3b), and the latter by setting $\tan v_1$, equal to Eq (3a) divided by Eq (3b), and determining the quadrant from the signs of numerator and denominator) The iteration continues until computed and observed times of flight agree to any preselected accuracy Of course, either Eq (4a), (4b), or (4c) is selected for the iteration depending upon whether e is less than, equal to, or greater than unity Having determined P, the parameter results from Eq (3c) Now one has sufficient information to determine the position and velocity vectors at the first observation time (and, thereby uniquely determine the two-body orbit) as discussed in Refs 1 and 2

Uniqueness Proof

The proof that the indicated procedure utilized yields one and only one value of P, e, and v_1, is as follows: Let the

Received October 31, 1963; revision received January 20, 1964

* Member of the Technical Staff, Trajectories Branch, Flight Mechanics Group Member AIAA
† Member of the Technical Staff, Trajectories Branch, Flight Mechanics Group

Table 1 Data combinations for self-contained preliminary orbit determination (after orientation of orbit plane and increment in true anomaly between observations $0 < \Delta v < \pi$ have been determined)

Data combination	Iteration required?	Comments
$r_1, \dot{r}_1, \dot{r}_2$	No	
$\dot{r}_1, r_1, r_2$	No	Under some circumstances, a measurement of $\dot{r}_2$ is required to remove ambiguities
$\dot{v}_1, \dot{r}_1, \dot{r}_2$	No	
$\dot{r}_1, \dot{v}_1, \dot{v}_2$	No	Under some circumstances, a measurement of $\dot{r}_2$ is required to remove ambiguities
$\dot{v}_1, r_1, r_2$	No	
$r_1, \dot{v}_1, \dot{v}_2$	No	
$\dot{v}_1\ \dot{v}_2, \dot{v}_3$	No	
r_1, r_2, r_3	No	Identical to classical Gibbsian method
$\dot{r}_1, \dot{r}_2, \dot{r}_3$		Yields no solution
$\dot{r}_1, \dot{r}_2, (t_2 - t_1)$	Yes	
$r_1, r_2, (t_2 - t_1)$	Yes	Identical to classical or modified Gaussian methods
$\dot{v}_1, \dot{v}_2, (t_2 - t_1)$	Yes	

subscripts a and b correspond to two orbits having identical values of Δv, $\dot{V}_1$ and $\dot{V}_2$ Then, from Eqs (2) and (3) at the observation times,

$$P_a\dot{V}_1 = 1 + e_a \cos v_{1a} \tag{5a}$$

$$P_a\dot{V}_2 = 1 + e_a \cos(v_{1a} + \Delta v) \tag{5b}$$

$$P_b\dot{V}_1 = 1 + e_b \cos v_{1b} \tag{5c}$$

$$P_b\dot{V}_2 = 1 + e_b \cos(v_{1b} + \Delta v) \tag{5d}$$

The time of flight is given by the integral[6]

$$t_2 - t_1 = P_a{}^2 \int_{v_{1a}}^{v_{1a}+\Delta v} \frac{dv_a}{(1 + e_a \cos v_a)^2} = P_b{}^2 \int_{v_{1b}}^{v_{1b}+\Delta v} \frac{dv_b}{(1 + e_b \cos v_b)^2} \tag{6}$$

Generalizing Eqs (5) for time t where $t_1 \leq t \leq t_2$ yields

$$P_a\dot{V}_a = 1 + e_a \cos v_a \qquad P_b\dot{V}_b = 1 + e_b \cos v_b$$

or

$$P_b{}^2 = P_a{}^2 \frac{dv_a}{dv_b}\left(\frac{1 + e_b \cos v_b}{1 + e_a \cos v_a}\right)^2 \tag{7}$$

Substituting (7) into the right-hand side of (6) yields

$$t_2 - t_1 = P_a{}^2 \int_{v_{1a}}^{v_{1a}+\Delta v} \frac{dv_a}{(1 + e_a \cos v_a)^2} = P_a{}^2 \int_{v_{1b}}^{v_{1b}+\Delta v} \frac{dv_a}{(1 + e_a \cos v_a)^2} \tag{8}$$

Since the integrands of both sides of Eq (8) are identical, the equation can be satisfied only if the integrand is a constant (indicating a circular orbit where v_{1a} and v_{1b} are arbitrary), or, if the limits satisfy the constraints

$$v_{1b} = v_{1a} \tag{9a}$$

or

$$v_{1b} = 2\pi - v_{1a} - \Delta v \tag{9b}$$

From Eqs (5),

$$\frac{\dot{V}_1}{\dot{V}_2} = \frac{1 + e_a \cos v_{1a}}{1 + e_a \cos(v_{1a} + \Delta v)} = \frac{1 + e_b \cos v_{1b}}{1 + e_b \cos(v_{1b} + \Delta v)} \tag{10a}$$

Substituting Eq (9b) into the preceding equation, yields

$$\frac{\dot{V}_1}{\dot{V}_2} = \frac{1 + e_a \cos v_{1a}}{1 + e_a \cos v_{1b}} = \frac{1 + e_b \cos v_{1b}}{1 + e_b \cos v_{1a}} \tag{10b}$$

Excluding the solution $e_a = e_b = 0$, where the true anomaly is arbitrary, Eq (10b) has two solutions:

$$\cos v_{1b} \neq \cos v_{1a} \qquad \cos v_{1a} + \cos v_{1b} = -1/e_a - 1/e_b \tag{11a}$$

and

$$\cos v_{1b} = \cos v_{1a} \tag{11b}$$

Since

$$\cos v_1 = \frac{1}{e_a}\left(\frac{p}{r_a} - 1\right) \qquad \cos v_{1b} = \frac{1}{e_b}\left(\frac{p}{r_b} - 1\right)$$

the solution given by Eq (11a) corresponds to the case where the vehicular separation from the dynamical center is infinite Since this case is of no practical interest, this solution is ignored Eq (11b) has two solutions:

$$v_{1b} = 2\pi - v_{1a} \tag{12a}$$

$$v_{1b} = v_{1a} \tag{12b}$$

Since substitution of Eq (12a) into Eq (9b) yields the indeterminate case where both solutions take place at the same time ($\Delta v = 0$), this solution can also be ignored The remaining solution given by Eq (12b) is identical to Eq (9a) Thus, the two orbits must have identical true anomalies at the first observation time Substitution of this condition into Eqs (5) yields $e_b = e_a$, $P_b = P_a$ Thus it is shown that the indicated procedure yields one and only one value of P, e, and v_1

Numerical Example

In order to test the method just presented, a selenocentric satellite orbit having the following characteristics is considered[2]: $a = 6{,}842{,}700$ ft, $e = 0\,1$, $\omega = 30°$, and $\Omega = 45°$, where a, ω, and Ω are the semimajor axis, argument of perise-lene, and argument of the ascending node, respectively It is further assumed that the sublatitude and sublongitude of the first observation are $\phi_1 = 30°$, $\lambda_1 = 90°$, and that the separation in true anomaly between the two observations is $\Delta v = 90°$ The preceding quantities uniquely determine the second set of sublatitude and sublongitude points and the time increment between observations as $\phi_2 = 22°\ 787$, $\lambda_2 = 193°\ 734$, and $t_2 - t_1 = 32\,918$ min, and the orbital inclination i as $i = 39°\ 232$

The simulated "measurements" of time rate of change of true anomaly associated with these "observations" are $\dot{v}_1 = 8\ 9043261 \times 10^{-4}$ rad/sec, and $\dot{v}_2 = 6\ 9055995 \times 10^{-4}$ rad/sec This orbit exhibits the following inertial components of position and velocity at the first observation time:

$$\mathbf{r}_1 \begin{cases} x_1 = 0 \\ y_1 = 5{,}369{,}700 \text{ ft} \\ z_1 = 3{,}100{,}200 \text{ ft} \end{cases} \qquad \dot{\mathbf{r}}_1 \begin{cases} \dot{x}_1 = -4938\ 1 \text{ fps} \\ y_1 = -1068\ 9 \text{ fps} \\ \dot{z}_1 = 2233\ 9 \text{ fps} \end{cases}$$

The simulated values of $\dot{v}_1$, ϕ_1, λ_1, $\dot{v}_2$, ϕ_2, λ_2, and $(t_2 - t_1)$ given previously are substituted into the equations derived in this paper (for determination of p, e, and v_1) and in Refs 1 and 2 (for determination of the orientation of the orbit plane in inertial space) In order to initiate the iteration procedure, the values $p = 8{,}370{,}400$ ft and $6{,}377{,}800$ ft were selected Two successive applications of Newton's iteration procedure yielded the following initial conditions

$$\mathbf{r}_1 \begin{cases} x_1 = 0 \\ y_1 = 5{,}368{,}200 \text{ ft} \\ z_1 = 3{,}099{,}300 \text{ ft} \end{cases} \qquad \mathbf{r}_1 \begin{cases} \dot{x}_1 = -4936\ 8 \text{ fps} \\ y_1 = -1065\ 0 \text{ fps} \\ z_1 = 2235\ 4 \text{ fps} \end{cases}$$

Conclusions

The results of Refs 1 and 2 and the present analysis are summarized in Table 1, where the symbols r, $\dot{r}$, and $\dot{v}$ corre-

spond to the distance from dynamical center, radial velocity, and time rate of change of true anomaly, respectively The first nine and last three data combinations listed correspond to types A and B, respectively

References

[1] Gersten, R H and Schwarzbein Z E "Self-contained orbit determination techniques," AIAA Preprint 63 431 (August 19–21, 1963)

[2] Schwarzbein Z E and Gersten R H, "Preliminary orbit determination for a moon satellite," AIAA J 1, 467–469 (1963)

[3] Herrick, S *Astrodynamics* (D Van Nostrand Company, Inc, Princeton, N J, in Press)

[4] Baker, R M L, Jr and Makemson, M W, *An Introduction to Astrodynamics* (Academic Press Inc, New York, 1960), Chap 6, pp 111–152

[5] Liu, A, Two body orbit determination from two positions and time of flight " Aeronutronic TN 4 (January 2, 1959)

[6] Plummer, H C, *An Introductory Treatise on Dynamical Astronomy* (Dover Publications, Inc, New York, 1960), pp 24–27

Effect of a Cavitating Venturi on Wave Propagation in a Duct

L R Iwanicki* and O W Dykema†
North American Aviation, Inc, Canoga Park, Calif

Introduction

A VENTURI designed to reduce the static pressure of the fluid flowing through the throat to its vapor pressure is termed a cavitating venturi When operating under this condition, assuming a constant upstream head, a decrease in pressure downstream of the venturi will not result in increased flow [1–4]

The purpose of this investigation, conducted for NASA, was to determine whether or not the cavitating venturi is effective in maintaining a constant flow when the downstream pressure oscillates in the frequency range of 100–1000 cps If the answer to this question is affirmative, this characteristic of the cavitating venturi could be useful when applied as a dynamic decoupling device in liquid rocket engines A logical location would be at the discharge end of the feed system to effectively decouple combustion and propellant feed system oscillations

Test System Configuration and Instrumentation

The function of the test system is to simulate the environment and boundary conditions that will exist in the actual application of the venturi To facilitate test programming, water was used as the test medium in conducting initial tests to study the effect of cavitating venturi action in a dynamic flow system Later, liquid oxygen replaced water to confirm that no serious deviations in this characteristic action resulted from a change in the test medium

A sketch of the test system configuration is shown in Fig 1 The system consists essentially of a 1-in -i d pipe, approximately 10 ft long, bounded at the upstream end by a large tank and terminated at the downstream end by an orifice discharging to the atmosphere A hydraulic siren, operating at a branch in the system immediately upstream of the discharge orifice, provides the oscillating hydraulic disturbance to the system during the dynamic tests The siren is capable of sweeping a continuous frequency range of 100–1000 cps when driven by a 5-hp, remotely controlled, d c variac motor

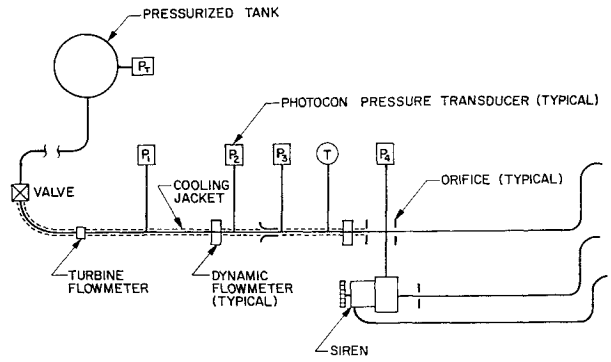

Fig 1 Test system configuration

Low pressure drop and effective fluid dynamic decoupling were desirable features for the intended venturi application According to Ref 5, the 7° diffuser included angle would insure a minimum pressure energy loss The venturi entrance contour was designed to have a radius, equal to twice the throat diameter, that would be conducive to efficient flow entry and at the same time leave more venturi length available for the diffuser The over-all length was limited by the space in the parent hardware

Instrumentation included Photocon pressure transducers to monitor the pressure oscillations, dynamic flowmeters (strain-gage, cantilever type) to record the oscillatory flow component, and Fastax camera recording equipment to determine the size and response of the cavitation bubble for variations in the pressure downstream of a lucite venturi A large electronic amplification is required to make the dynamic flow data measurable Amplification was accomplished *before* the flow signal was recorded on tape so that further amplification before playback was held to a minimum, thus limiting amplification of the tape noise

Test Procedure

With the system fluid flowing through the venturi under the prescribed tank pressure of 1500 psi, the siren was operated over the full-frequency range of interest, 100–1000 cps, with all transducer outputs being recorded on tape for later analysis Only oscillatory components of the pressure and flow

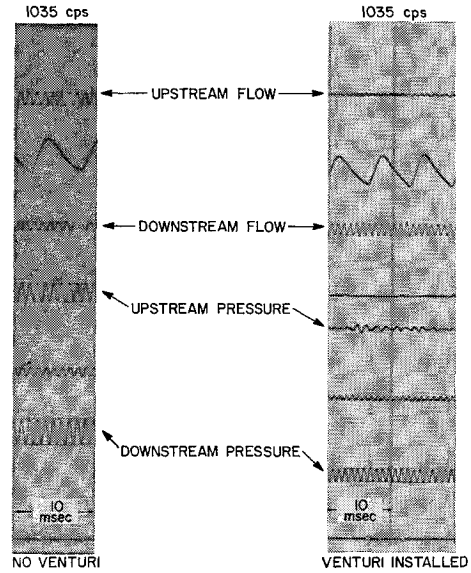

Fig 2 Typical filtered traces

Received September 3, 1963; revision received January 27, 1964

* Research Specialist, Liquid Rocket Engineering Department, Rocketdyne Division Member AIAA

† Supervisor, Liquid Rocket Engineering Department, Rocketdyne Division